



Ship Technology Research

Schiffstechnik

ISSN: (Print) (Online) Journal homepage: <https://www.tandfonline.com/loi/ystr20>

A new power prediction method using ship in-service data: a case study on a general cargo ship

Ehsan Esmailian, Young-Rong Kim, Sverre Steen & Kourosh Koushan

To cite this article: Ehsan Esmailian, Young-Rong Kim, Sverre Steen & Kourosh Koushan (01 Nov 2023): A new power prediction method using ship in-service data: a case study on a general cargo ship, Ship Technology Research, DOI: [10.1080/09377255.2023.2275378](https://doi.org/10.1080/09377255.2023.2275378)

To link to this article: <https://doi.org/10.1080/09377255.2023.2275378>



© 2023 The Author(s). Published by Informa UK Limited, trading as Taylor & Francis Group



Published online: 01 Nov 2023.



Submit your article to this journal [↗](#)



Article views: 580




View related articles [↗](#)



View Crossmark data [↗](#)

A new power prediction method using ship in-service data: a case study on a general cargo ship

Ehsan Esmailian ^{a,b}, Young-Rong Kim^{a,c}, Sverre Steen^a and Kourosh Koushan^{a,d}

^aDepartment of Marine Technology, Norwegian University of Science and Technology (NTNU), Trondheim, Norway; ^bKumera Marine AS (Hjelseth), Hjelset, Norway; ^cDepartment of Mechanics and Maritime Sciences, Chalmers University of Technology, Gothenburg, Sweden; ^dDepartment of Ship and Ocean Structures, SINTEF Ocean AS, Trondheim, Norway

ABSTRACT

To increase energy efficiency and reduce greenhouse gas (GHG) emissions in the shipping industry, an accurate prediction of the ship performance at sea is crucial. This paper proposes a new power prediction method based on minimizing a normalized root mean square error (NRMSE) defined by comparing the results of the power prediction model with the ship in-service data for a given vessel. The result is a power prediction model tuned to fit the ship for which in-service data was applied. A general cargo ship is used as a test case. The performance of the proposed approach is evaluated in different scenarios with the artificial neural network (ANN) method and the traditional power prediction models. In all studied scenarios, the proposed method shows better performance in predicting ship power. Up to 86% percentage difference between the NRMSEs of the best and worst power prediction models is also reported.

ARTICLE HISTORY

Received 20 December 2022
Accepted 16 July 2023

KEYWORDS

Power prediction; in-service data; GHG emission; artificial neural networks (ANN); ship performance

Nomenclature

A_E/A_0	expanded area ratio
A_{xv}	transverse projected area above the waterline
C_{AA}	wind resistance coefficient
C_B	block coefficient
C_M	midship section coefficient
C_{WP}	waterplane area coefficient
d	ship draft
D_p	propeller diameter
g	gravity acceleration
H_s	significant wave height
J	advance coefficient
K_Q	torque coefficient
K_T	thrust coefficient
L_{pp}	length between perpendiculars
n	number of samples
n_p	rotational speed of the propeller in Hz
n_{rpm}	propeller rpm
P/D_p	pitch ratio
P_{AW}	added power in waves
P_{aux}	auxiliary power
P_{Calm}	calm water power
P_s	shaft power
P_{sopr}	operation shaft power
P_{Scal}	calculated shaft power
P_{tot}	total power
P_{Wind}	added power due to the wind
R_{aw}	added resistance in waves
R_{Calm}	calm water resistance
R_{Wave}	added resistance in irregular waves
R_{Wind}	added resistance due to the wind
R_T	total resistance
s	power exponent

t	power exponent
T_p	peak wave period
u	power exponent
v	power exponent
V_A	advance velocity
V_d	design speed
V_G	ship speed over ground
V_S	ship forward speed
V_{WRref}	relative wind velocity at the reference height
V_{WTref}	corrected true wind velocity
w	wake factor
Z	number of blades
β	encounter wave angle
η_D	quasi-propulsive efficiency
η_H	hull efficiency
η_o	open water efficiency
η_R	relative rotative efficiency
η_S	shaft efficiency
η_P	total propulsive efficiency
∇	ship displacement volume
ω	wave frequency
ψ	ship heading
ψ_{WRref}	relative wind direction at the reference height
ψ_{WT}	true wind direction
ρ_A	density of air
ζ_a	wave amplitude

1. Introduction

The shipping industry contributes between 2-3% of total carbon emissions worldwide. By the year 2050, it is projected that the greenhouse gas (GHG) emissions from the maritime industry will experience an

CONTACT Ehsan Esmailian  ehsan.esmailian@ntnu.no, eh.esmailian@gmail.com  Kumera Marine AS (Hjelseth), Baklivegen 11-13, 6450 Hjelset, Norway

© 2023 The Author(s). Published by Informa UK Limited, trading as Taylor & Francis Group
 This is an Open Access article distributed under the terms of the Creative Commons Attribution-NonCommercial-NoDerivatives License (<http://creativecommons.org/licenses/by-nc-nd/4.0/>), which permits non-commercial re-use, distribution, and reproduction in any medium, provided the original work is properly cited, and is not altered, transformed, or built upon in any way. The terms on which this article has been published allow the posting of the Accepted Manuscript in a repository by the author(s) or with their consent.

increase ranging from 50% to 250% (Smith et al. 2015). For a more effective analysis of these trends, it is essential to have knowledge of typical marine emission modelling techniques and their respective impacts. In addition, the estimation of GHG emissions in the shipping industry and evaluation of their effects on climate play a vital role in the development of regulations, identifying the most effective solutions for mitigating emissions, and making well-informed decisions concerning the reduction of emissions in the future. All activity-based marine emission models encompass an estimate of ship propulsive power, for which an array of methods with varying levels of complexity are available. However, the influence of ship power models on marine emissions inventories has not received much focus while significant differences in the results of different power prediction models have been reported (Brown and Aldridge 2019).

A power prediction model is applied for a variety of applications, including ship and propeller design (Esmailian et al. 2019, 2017), weather routing (Kim and Kim 2017; Shao et al. 2012), fleet performance analysis (Vernengo et al. 2016; Kim et al. 2023), modelling and analysis of the ship propulsion system (Saettone et al. 2020; Tadros et al. 2021), energy management of the ship power system (Planakis et al. 2022), modelling the ship emission and the fuel consumption (Wang and Rakha 2017; Kim et al. 2021), hull condition monitoring (Koboević et al. 2019), and other operational optimization purposes (Sun et al. 2013; Tillig et al. 2020). Over the past few decades, a large number of research have been published suggesting methods to compute different components of a power prediction model, including calm water resistance (Guldhammer and Harvald 1974; Holtrop 1984; Hollenbach 1998; Kristensen and Lützen 2012), added resistance due to waves (Faltinsen 1980; ISO 2015; Grin 2015), added resistance due to winds (Blendermann 1995; Watson 1998; ISO 2015; Kitamura et al. 2017), propulsion system efficiency (Oosterveld and van Oossanen 1975; Schneekluth and Bertram 1998; ITTC 2014), and so on. Along with this, there has been a growing number of power prediction models using regression formulas in recent years (Kristensen and Lützen 2012; Johansson et al. 2017; Tillig et al. 2018). They require low computational time and cost. However, the accuracy of the predicted power might vary substantially from ship to ship depending on the methods used to calculate the different components of the power prediction model.

Ships are increasingly equipped with data acquisition systems onboard. The data can be utilized by shipowners, operators, as well as ship designers to improve vessel performance at sea. In the past few years, a large number of machine-learning methods have been also proposed to predict ship power at sea

using the ship in-service data (Petersen et al. 2012; Beşikçi et al. 2016; Parkes et al. 2018; Zhang et al. 2019; Moreira et al. 2021). However, the effectiveness of this category of power prediction models is highly dependent on the amount and quality of the training data. Machine learning models are also notoriously bad at extrapolation, meaning that the training data must properly cover the entire range of validity of the model. In-service data tends to provide an ample amount of data only for normal service conditions, while prediction of the power requirement for off-design conditions is often desired. Further, machine learning models are typically thought of as “black boxes,” with users having little to no understanding of the reasons behind a prediction. In this case, by providing a certain level of explainability for the model, users’ confidence in the models can increase (Shin 2021).

Numerical methods, i.e., CFD simulations validated against the results of a model test, are traditionally used to predict ship power (Lee et al. 2021). However, they require a lot of time and resources, as well as access to detailed ship and propeller geometry information. Also, they require an experienced user to calculate reliable results.

In conclusion, a wide variety of methods can be used to predict ship power. Each method has its own pros and cons, and thus its applicability and accuracy would vary depending on the ship type and the application scenario. However, despite having access to a variety of prediction methods, the shipping industry still lacks a quantification of the expected prediction accuracy and an understanding of possibilities for improving the accuracy (Tillig et al. 2018). In addition, it is still quite challenging to find proper methods and input parameters for calculating different components of a power prediction model for a given ship.

In this study, we propose a new method based on the use of ship in-service data to obtain the best combination of existing methods and their input parameters for calculating different components of a power prediction model, with the goal of improving the accuracy of the power prediction model for a given ship. For this purpose, a normalized root mean square error (NRMSE) is defined by comparing the results from the power prediction model with the ship in-service data of a reference vessel. Then, a tuning surrogate-based optimization problem is developed to minimize the NRMSE and find the optimal combination of existing methods and input parameters used to compute different components of the ship power (calm water resistance, added resistance in wind and wave, wetted surface, wake, etc.). In this way, the optimum combination of existing elements of the power prediction method can be applied. Since the method requires access to in-service data, it is applicable in cases where there is a need for a

good and robust powering prediction method for a ship already in operation. This could be for weather routing, hull condition monitoring, and other operational optimization purposes. It is also likely that using the method to predict the performance at an early design stage of a ship quite similar to the ship for which in-service data exists would work. The proposed method is tested on a general cargo ship operating on a route between Italy and Norway. In addition, the performance of the proposed approach is evaluated for different missions and voyages. It is also compared with the artificial neural network (ANN) method under the studied operational scenarios. An investigation is conducted into the effects of the sampling time interval and the length of time history on the performance of the proposed approach and ANN method. Finally, a comparison is made with conventional power prediction models proposed by Lindstad et al. (2013), Johansson et al. (2017), and Kristensen et al. (2017).

The suggested method is described in Section 2. The proposed method is implemented on a general cargo ship as a test case in Section 3. Comparisons between the ANN and traditional methods are presented in Section 4. Section 5 contains the conclusion.

2. Proposed method

The main idea behind the proposed method is the use of ship in-service data to obtain the best combination of existing methods and their input parameters. The implementation of the suggested power prediction method can be divided into four steps, as follows:

Step 1. Select a target ship

The proposed method is theoretically applicable to different ship types and application scenarios as long as the in-service data for the studied ship or a similar ship is available. Also, it might be applied to other types of performance data than in-service data as long as the performance data is accurate and covers a large enough range of variation in the involved parameters.

In the proposed method, we are considering two essential categories of inputs; ship data and environment data. Combining these two inputs provides a more complete picture. The first one gives us an insight into what was happening on the ship, and the second tells us about the environmental conditions the ship was facing. It should be noted that the inputs depend on which candidate methods are included in the proposed method in *Step 3*. The details of those inputs are discussed below.

- *Ship Data*: This includes information from the ship hull and propeller (length, breadth, depth, propeller

diameter, pitch ratio, number of blades, geometry, etc.) and ship in-service data. The ship's in-service data includes information collected by a number of sensors placed on the ship. Table 1 displays a typical categorized list of all the different types of data recorded on a ship. These variables are divided into several categories, each representing a specific type of information about the ship. The categories are:

- Ship Identity – Information that identifies the ship, including the ship name and IMO number.
- Navigation – Information related to the ship's course and position.
- Auxiliary Power System – Information about the ship's supporting power systems.
- Propulsion System – Information related to the propulsion system, such as shaft speed and power.

There is also 'Time', which is kept separate and considered its own variable. Navigation data is used to interpolate historical weather data, representing the environmental loads acting on the ship. In this study, shaft power is the focus, and data about the auxiliary power system is irrelevant.

Variables related to the propulsion system are mainly associated with the ship's hydrodynamic performance. The 'State' variable specifies the operational status of the vessel at any given moment, with one of the following four values for each time step: 'At Berth', 'Manoeuvring', 'Sea Passage', or 'Anchor/Waiting'. Only data labelled 'Sea Passage' is used for the analysis in this study. In addition, the Shaft Power and Shaft Rpm are inputs to the power prediction method. 'Draft Fore' and 'Draft Aft' variables are utilized to create two additional

Table 1. A typical list of variables recorded onboard the ship. Abbreviations: IMO = International Maritime Organization; COG = Center of Gravity; Aux. = Auxiliary; DG = Diesel Generator (for auxiliary power systems); ME = Main Engine (for propulsion system); GPS = Global Positioning System (Gupta et al. 2021).

Ship Identity	Navigation	Auxiliary Power System	Propulsion System
Ship Name	Latitude	Aux. Consumed	State
IMO Number	Longitude	Aux. Electrical Power Output	ME Load Measured
	Gyro Heading	DG1 Power	Shaft Power
	COG Heading	DG2 Power	Shaft Rpm
			Shaft Torque
			ME Consumed
			Draft Fore
			Draft Aft
			GPS Speed
			Log Speed
			Cargo Weight

variables: mean draft and trim-by-aft, which are more pertinent from a hydrodynamics perspective. The effects of the cargo weight are accounted for by taking into consideration the variations in the ship's draft.

There is often a debate regarding whether to utilize speed through water (known as log speed) or speed over the ground (known as GPS speed) for analysis (Gupta et al. 2022). It is a well-recognized fact that the measurement of speed through the water is only somewhat reliable. This is because the flow of water passing through the device can be altered by the ship's hull or by various environmental conditions. However, it is widely acknowledged that GPS speed measurements are more reliable since GPS sensors have become highly accurate in recent times. However, log speed is more applicable for hydrodynamic analysis as it reflects the actual speed of the ship through the water, which is directly associated with the effective power of the propeller. The difference between GPS and log speed arises due to the speed of the longitudinal sea current. In the absence of any sea current, the GPS and log speeds should coincide. However, when there is a lack of reliable log speed data and the impact of the current is substantial, it could be advantageous to incorporate GPS speed measurements into the analysis, coupled with reliable data on the longitudinal water current speed from the hindcast.

- *Environment Data*: It contains the environment's constant parameters and weather hindcast data. Constant parameters, such as salinity and water density, can affect ship buoyancy, resistance, and propulsion efficiency. The weather hindcast data (also known as metocean data) contains information about the weather conditions that the ship likely encountered during its journey. It is gathered from three publicly accessible sources, namely: (a) European Centre for Medium-Range Weather Forecasts (ECMWF) (ECMWF 2017), (b) Hybrid Coordinate Ocean Model (HYCOM) (Chassignet et al. 2007), and (c) Copernicus Marine Environment Monitoring Service (CMEMS) (CMEMS 2018). These sources offer data variables that encompass information related to the three principal environmental loads – wind (obtained from ECMWF), waves (also from ECMWF), and sea currents (sourced from either HYCOM or CMEMS). Additionally, information on geoid depth at sea is procured from CMEMS.

In this study, the historical weather data, which includes information on wind and waves, is gathered from the ECMWF, specifically from its Copernicus Climate Change Service (C3S). The data from ECMWF is sourced from the ERA5 High Resolution

(HRES) climate reanalysis dataset. In this context, ERA5 HRES has a spatial resolution of 0.25 degrees, meaning the data points are spaced 0.25 degrees apart, and a temporal resolution of 1 hour, meaning the data is updated every hour. The weather data elements are adjusted both in terms of location and time to match the ship's position using the available navigation data through a process called linear interpolation.

Step 2. Data preprocessing

Data preprocessing is a data mining technique used to turn raw data into a useful and efficient form. This technique consists of cleaning up raw data sets by removing outliers or noise that are inappropriate for analysis before implementing a model. In this study, the method presented by Gupta et al. (2021) is used for the data preprocessing.

Step 3. Select candidate methods and parameters

This step aimed at selecting the alternative procedures for calculating different aspects of the power prediction model, such as the wetted surface area, the added resistance in wind and waves, the calm water resistance, the propulsion system efficiency, etc. Several factors, such as applicability to a wide range of ship types, high accuracy, computational efficiency, and low numbers of inputs, should be taken into account while selecting the candidate method. The user might need to select different candidate methods, parameters, and assumptions, depending on the ship in question. The selection of methods provided in the case study in Section 3 is believed to be appropriate for many normal merchant vessels, but in order to apply the proposed methodology to, for instance, high-speed ships, quite different candidate methods are needed.

Step 4. Implement the proposed power prediction method

The general flowchart of the proposed approach is presented in Figure 1. The aim is to use the ship's in-service data to obtain the best combination of the candidate methods and parameters to reach more accurate power prediction models. The inputs depend on which candidate methods are included in the proposed method from **Step 3**. Additionally, the selection of the methods and parameters is based on the user's expectations for reaching desired error margins and limitations in computational time. Nevertheless, it goes without saying that including a greater number of input parameters and methods increases the likelihood of achieving more accurate power prediction models. The calculated shaft power (P_{sCal}) in different

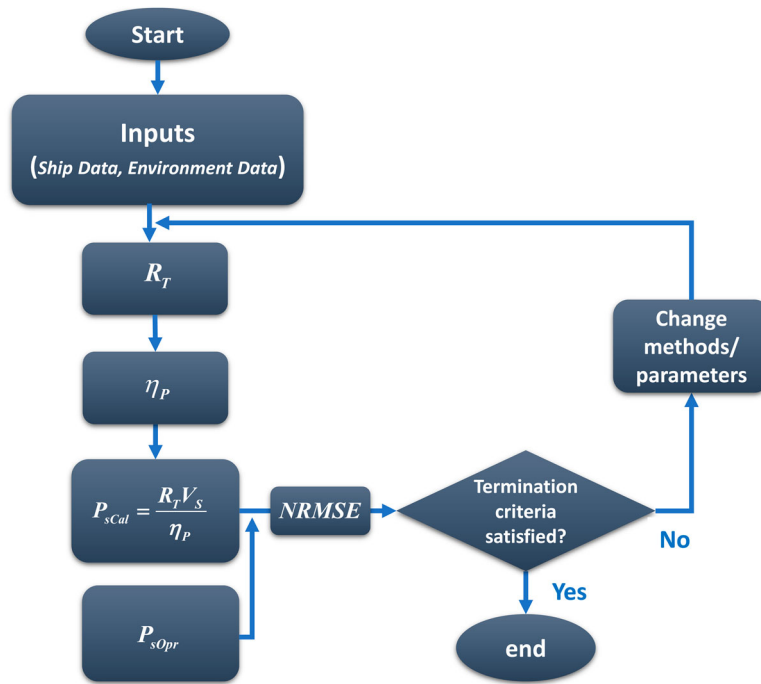


Figure 1. The flowchart of the proposed power prediction method.

speeds (V_S) is determined as follows.

$$P_{sCal} = \frac{R_T V_S}{\eta_p}$$

where R_T and η_p are the total resistance and total propulsive efficiency, respectively. Error in a dataset can be evaluated with a variety of metrics, such as mean absolute error (MAE), root mean square error (RMSE), mean square error (MSE), and normalized root mean square error (NRMSE). When evaluating the performance of a model, RMSE is commonly preferred to MAE. This is due to the fact that RMSE is more useful as users frequently aim to minimize the occurrence of large outliers in their predictions, and MAE may be viewed as overly simple for assessing overall model performance. Large prediction errors are also penalized by the Mean Square Error (MSE). But it is more common to use RMSE over MSE because it is measured in the same units as the response variable. A ship might experience different ranges of power in different voyages over the ship's entire operation. To be able to compare the performance of the power prediction model among different voyages, the NRMSE that is scale-free is favoured over the RMSE for comparison of the performance of

the power prediction model among different voyages. Then normalization is done on the maximum continuous rating (MCR) of the engine, which is defined as the maximum continuous power at the engine's maximum continuous rotation rate. Now, knowing the calculated power P_{sCal} and the shaft power from ship in-service data, the NRMSE is determined as follows.

$$NRMSE(X) = \frac{RMSE(X)}{MCR}$$

with

$$RMSE(X) = \sqrt{\frac{\sum_{i=1}^n (P_{sCal}(X) - P_{sOpr})^2}{n}}$$

where n is the number of samples. Also, X is the vector of the decision variables, including the candidate methods and input parameters selected in Step 3. In this study, the Matlab surrogate optimization method is used as the optimization algorithm to minimize the NRMSE, which is recommended for time-consuming objective functions (MathWorks 2022). Table 2 presents the optimization settings that correspond to Matlab's default settings. The tuning process terminates when it exceeds the function evaluation limit. During the optimization process, different candidate methods and parameters are evaluated by the optimization algorithm to find the best combination of methods and parameters that corresponds to the minimum value of the NRMSE and thus the highest accuracy of the power prediction model. The surrogate optimization method is applicable for solving problems of the form

Table 2. Optimization algorithm settings.

Option	Value
Batch Update Interval	1
Constraint Tolerance	1e-3
Max Function Evaluations	max(20, 5*nvar)
Max Time	Inf
Min Sample Distance	1e-6
Min Surrogate Points	max(20, 2*nvar)



Figure 2. The ship operational route for Mission 1.

MathWorks (2022)

$$\min_X f(X) \text{ such that } \begin{cases} AX \leq b & \text{(inequality constraint)} \\ A_{eq}X = b_{eq} & \text{(equality constraint)} \\ c(X) \leq 0 & \text{(nonlinear inequality constraint)} \\ lb \leq X \leq ub & \text{(bound constraint)} \\ X_i \in Z & \text{(integer constraint)} \end{cases}$$

In this study, $f(X) = NRMSE(X)$.

3. Case study

Step 1. Select a target ship

Here, the proposed method is tested on a general cargo ship operating on a route between Italy and Norway (Figure 2) referred to as Mission 1. Mission 1 is considered as the main mission of the ship. Table 3 provides the main particulars of the general cargo ship.

The studied ship is seven years old and data on its ship-in-service condition are automatically collected with a sampling frequency of 15 minutes almost throughout the entire operation. For location data, the Automatic Identification System (AIS) database is used. The ECMWF database is used for the weather hindcast data. The shaft power, shaft rpm, mean

Table 3. Main particulars of the general cargo ship.

Parameters	Value
Ship type	General cargo
Length [m]	194
Breadth [m]	32
Block coefficient [–]	0.8
Design draught [m]	12.6
Service speed [knots]	15.5

draft, ship speed, significant wave height, peak wave period, and encounter wave angle (obtained based on the difference between the mean wave direction and ship heading) are the inputs to the power prediction model.

Step 2. Data preprocessing

Here, the data preprocessing is carried out using the method presented by Gupta et al. (2021).

Step 3. Select candidate methods and parameters

Here, the candidate method and parameter selections for the proposed method are discussed. The main goal is to assess the performance of the suggested method for providing more accurate power prediction models. However, the proposed approach can be broadened to incorporate more elements and approaches than those applied in this study based on the user's decision to provide even better results. The selection of methods provided here is believed to be appropriate for many normal merchant vessels, but in order to apply the proposed methodology to, for instance, high-speed ships, quite different candidate methods are needed.

3.1. Resistance

Previous studies have mostly focused on assessing the ship performance in the calm water condition, despite

the fact that ships seldom operate in calm water and that their performance may vary significantly in the actual sea states. It is therefore necessary to calculate the added resistance based on the ship's operational conditions. The added resistances due to waves and winds are taken into account in this study. Consequently, the ship's total resistance is formulated as follows.

$$R_T = R_{Calm} + R_{Wave} + R_{Wind}$$

where R_{Wave} , R_{Wind} , and R_{Calm} stand for the added resistance brought on by waves, the wind, and the calm water resistance, respectively. The added resistance will also be caused by maneuvering and rudder effect. However, these are often not as important and are thus disregarded in the present work.

3.1.1. Calm water resistance

For estimating the calm water resistance, the revised Guldhammer-Harvald's (GH) (2017), Holtrop-Mennen's (HM) (1984), and Hollenbach's (HB) (1998) techniques are taken into account. Those methods, which are still widely used today, provide regression-based equations resulting from comprehensive model testing analyzes. Since Holtrop-Mennen's approach has the broadest applicability, it should be included. Studies conducted by Hollenbach suggest that Holtrop-Mennen's and Hollenbach's methods are more accurate than the original Guldhammer-Harvald's model. Hence, Hollenbach's and Holtrop-Mennen's methods are both included. However, it is acceptable to add the improved version of Guldhammer-Harvald's approach because it fits modern ships, as noted by Kristensen et al. (2017). Holtrop-Mennen's method has fewer limitations compared to Guldhammer-Harvald's and Hollenbach's. However, it is believed that all three are applicable to typical cargo ships. Here, Hollenbach's method is applied using the mean line. The mean values of GH & HM, GH & HB, and HM & HB combinations are also included in the tuning process.

The average hull roughness (AHR) for a new ship usually falls within the range of 75 to 125 μm . In this study, when calculating the resistance in calm waters, an AHR of 150 μm is used, including the effects of fouling. This 150 μm is the standard value that ITTC suggests using in cases where there is no available measured data (ITTC 2014). This assumption is based on the fact that ship-in-service data are studied within a short period, wherein the effects of the change in fouling are not significant. For a long-term analysis of the power prediction model, the in-service performance data should preferably be corrected for the effect of changing levels of roughness and fouling.

3.1.2. Added resistance in waves

The mean added resistance in the irregular waves is determined by numerically integrating a sequence of regular waves with frequency ω and wave amplitude ζ_a for a given peak wave period T_p , encounter wave angle β , and the significant wave height H_s . It is expressed as

$$R_{AW} = 2 \int_0^{2\pi} \int_0^\infty S(\omega, H_s, T_p) \frac{R_{aw}(\omega, \beta, V_S)}{\zeta_a^2} d\omega d\beta$$

where V_S , S , and R_{aw} denote the ship speed, the wave spectrum, and the frequency-dependent added resistance due to waves, respectively. The encounter wave angle β can be obtained based on the mean wave direction and navigation data (latitude and longitude coordinates of the ship). In the present work, the modified Pierson-Moskowitz (Bretschneider) wave spectrum is used (Perez 2006). In the literature, there are several ways to calculate R_{aw} . STA-1 and STA-2 are suggested by ISO 15016, while the STA-1 method is for moderate sea conditions (ISO 2015). Then, STA-2 was suggested to improve its applicability in higher sea states. However, both STA-1 and STA-2 are solely applicable for head seas (+ – 45 degrees off the bow). Different techniques, including CTH (Lang and Mao 2021), SNNM (Liu and Papanikolaou 2020), and Combined (Kim et al. 2022) approaches, have recently been developed. These techniques outperformed STA2 substantially in almost all comparison scenarios, and they also have the benefit of being able to estimate R_{aw} for arbitrary wave headings. They also only need a limited number of hull data. CTH, SNNM, and Combined techniques are therefore used in the tuning approach. There are undoubtedly numerous numerical techniques for calculating added resistance in waves. However, the present study does not use any of them due to the general need for comprehensive meshing, high computational time, and possible lack of robustness.

3.1.3. Added resistance due to wind

The total resistance might be significantly increased for ships with large volumes above the waterline due to the added wind resistance. The added resistance due to wind can be written as ISO (2015).

$$R_{wind} = 0.5\rho_A \cdot C_{AA}(\psi_{WRref}) \cdot A_{xv} \cdot V_{WRref}^2 - 0.5\rho_A \cdot C_{DA}(0) \cdot A_{xv} \cdot V_G^2$$

where $C_{AA}(\psi_{WRref})$ is the wind resistance coefficient, wherein ψ_{WRref} is the relative wind direction at the reference height (usually 10 meters above the free surface). Also, ρ_A , A_{xv} , V_G , and V_{WRref} are the air density, the transverse projected area above the waterline, the ship speed over the ground, and the relative wind velocity at the reference height, respectively. Here, $V_G =$

V_S . V_{WRref} is expressed as

$$V_{WRref} = \sqrt{V_{WTref}^2 + V_G^2 + 2 \cdot V_{WTref} \cdot V_G \cdot \cos(\psi_{WT} - \psi)}$$

where V_{WTref} , ψ_{WT} , and ψ denote the corrected true wind velocity, true wind direction, and the ship heading, respectively. More details about this method can be found in (ISO 2015). In this study, it is assumed that the wind and wave are both pointing in the same direction for simplification. Thus, $\beta = \psi_{WT} - \psi$. However, the user can replace each with more accurate information depending on the situation. Also, V_{WTref} is given by Stewart (2008):

$$V_{WTref} = \sqrt{\frac{gH_s}{0.22}}$$

where g is the gravity acceleration. Model tests in a wind tunnel, CFD analysis, or coefficients derived from tabular data, which are frequently based on previous research with comparable ship forms, can be used to predict the wind resistance coefficients C_{AA} . It is known that Blendermann (1995) and ISO 15016 (ISO 2015) might provide accurate estimations of wind resistance coefficients in the absence of wind tunnel measurements. Therefore, these two techniques are part of the tuning strategy in this work.

3.2. Propulsion system

The overall propulsive efficiency η_p is calculated as

$$\eta_p = \eta_D \eta_S$$

where η_S is the shaft efficiency. Also, η_D is the quasi-propulsive efficiency and is defined as

$$\eta_D = \eta_H \eta_o \eta_R$$

where η_H , η_o , and η_R are the hull efficiency, the open water efficiency, and the relative rotative efficiency, respectively. The Wageningen B-series method is frequently used to assess propeller performance during the early phase of the estimation of the open water efficiency Oosterveld and van Oossanen (1975). These non-ducted fixed pitch propellers range in blade area ratios from 0.30 to 1.05, pitch ratios from 0.5 to 1.4, and blade numbers from 2 to 7. Polynomials based on a regression analysis of the test results of 120 B-screw series propeller models are used to express the open water characteristics of the Wageningen B-series propellers as follows.

$$K_T = \sum C_{s,t,u,v}^T (J)^s \left(\frac{P}{D_p}\right)^t \left(\frac{A_E}{A_o}\right)^u (Z)^v$$

$$K_Q = \sum C_{s,t,u,v}^Q (J)^s \left(\frac{P}{D_p}\right)^t \left(\frac{A_E}{A_o}\right)^u (Z)^v$$

where J , P/D_p , A_E/A_o , and Z are the advance

coefficient, the pitch ratio, the blade expanded area ratio, and the number of blades, respectively. Further, based on the information provided in Oosterveld and van Oossanen (1975), the regression coefficients $C_{s,t,u,v}^Q$ and $C_{s,t,u,v}^T$ and exponents s , t , u , and v are determined. The expression for the advance coefficient, J , is

$$J = \frac{V_A}{n_p D_p}$$

with

$$V_A = V_S(1 - w).$$

where w is the wake factor. The open water efficiency is expressed as follows:

$$\eta_o = \frac{K_T J}{K_Q 2\pi}.$$

Knowing the propeller parameters, the ship speed, the wake factor, and the propeller revolution rate, the open water efficiency can be obtained from Equation (16). The wake factor, the thrust deduction factor, and the relative rotative efficiency are calculated using the formulas and assumptions given in the respective resistance prediction method (e.g. if Holtrop's method is used for resistance, the formulas for the wake, thrust deduction, and relative rotative efficiency given in that method are applied). Even though operation in waves may have an impact on the wake and thrust deduction factors, this effect is not taken into consideration here. Also, it is assumed that the shaft efficiency is $\eta_S = 0.98$ (Kristensen et al. 2017).

For the full-scale vessel, it is not recommended to use the same K_T and K_Q values as those used in the open water test. The Reynolds number of model propellers is often less than that of full-scale propellers and thus there is a difference in the turbulence level of the model and full scale. The thrust and torque coefficient polynomials should thus be modified to take the full-scale Reynolds number into account. The ITTC method (ITTC 2014), which calculates full-scale thrust and torque, can be used to make the correction as follows-

$$K_{T_s} = K_T - \Delta K_T$$

$$K_{Q_s} = K_Q - \Delta K_Q$$

where the procedure to calculate the corrections of ΔK_T and ΔK_Q is presented in ITTC (2014). There are also a number of well-known empirical methods that have been developed to assess propulsive efficiency as follows.

Auf'm Keller formula (Schneekluth and Bertram 1998):

$$\eta_D = 0.885 - 0.00012 \cdot n_{rpm} \cdot \sqrt{L_{pp}}$$

Table 4. Candidate methods for different decision variables.

R_{Calm}	R_{Wave}	R_{Wind}	η	S_{wet}	C_M	C_{WP}
Holtrop-Mennen (HM)	SNNM	Blendermann	B-series	Mumford's formula	Schneekluth and Bertram	Papanikolaou
Hollenbach (HB)	CTH	ISO 15016	B-series with ITTC correction	Num. computation	Num. computation	Num. computation
Guldhammer-Harvald (GM)	Combined		Auf'm Keller			
mean (HB & HM)						
mean (HB & GM)						
mean (GM & HM)						

Emerson's formula (Watson 1998):

$$\eta_D = 0.84 - \frac{n_{rpm} \cdot \sqrt{L_{pp}}}{10000}$$

where n_{rpm} and L_{pp} are the propeller rpm and the length between perpendiculars. According to Watson (1998), Emerson's formula applies to different ship types and is derived for low propeller speeds, but has been extended to modern propellers. Auf'm Keller's formula is applicable for cargo and passenger ships. Thus, the B-screw series formulas, the B-screw series formulas with ITTC full-scale correction procedure, the Auf'm Keller formula, and Emerson's formula are applied in the tuning process.

3.3. Hydrostatic parameters

Numerical methods or regression-based formulas can be used to calculate a ship's hydrostatic characteristics. Here, the wetted surface area (S_{wet}), midship section coefficient (C_M), and waterplane area coefficient (C_{WP}) are considered in the proposed method. These parameters fall into the group of input parameters usually derived either numerically or via regression in the literature. Therefore, it is interesting to explore the impact of this selection on the performance of the power prediction model. Hence, even though the ship offset table is available for the studied ship and is utilized for numerical calculations, hydrostatic parameters such as S_{wet} , C_{WP} , and C_M are also computed using the regression-based method with the aim of providing a comparative analysis. Then, the following well-known regression-based formulae are considered in this study:

Mumford's formula (Kristensen and Lützen 2012):

$$S_{wet} = 1.025 \cdot \left(\frac{\nabla}{d} + 1.7 \cdot L_{PP} \cdot d \right)$$

Table 5. Bounds of the design variables vector.

	Lower limit	Upper limit
$i_{R_{Calm}}$	1	6
$i_{R_{Wave}}$	1	3
$i_{R_{Wind}}$	1	2
i_{η}	1	3
$i_{S_{wet}}$	1	2
i_{C_M}	1	2
$i_{C_{WP}}$	1	2

Papanikolaou (2014):

$$C_{WP} = \frac{1 + 2C_B}{3}$$

Schneekluth and Bertram (1998):

$$C_M = 0.93 + 0.08C_B$$

where C_B , ∇ and d are the block coefficient, the ship displacement volume, and the ship draft, respectively. Other hydrostatic parameters are obtained numerically using the ship offset table.

Step 4. Determination of the optimum power prediction method

As mentioned earlier, power prediction models rely on predetermined assumptions, which may adversely affect the accuracy of the power prediction models. This section aims to present an example that demonstrates the potential of the proposed method for achieving more accurate power prediction models, as well as examining the impact of assumptions typically used in such models. To this end, Model 1 is formulated to assess the potential of the proposed approach in achieving the optimal power prediction model. Meanwhile, Model 2 is designed to evaluate the negative effects of these assumptions and determine how the prediction accuracy differs between the worst and best models.

In this example, seven components – namely, R_{Calm} , R_{Wave} , R_{Wind} , η , S_{wet} , C_M , and C_{WP} – are considered. Candidate methods for each of these components are defined and are listed in Table 4. To incorporate candidate methods into the optimization process, each candidate method of every component is assigned a unique integer. The bounds of these

Table 6. Constant parameters (x_{const}) in the optimization problem.

Parameters	Definition	Value	Unit
A_E/A_o	Expanded area ratio	0.54	–
D_p	Propeller diameter	7.00	m
g	Gravity acceleration	9.81	m/s ²
P/D_p	Pitch ratio	0.83	–
Z	Number of blades	4	–
η_R	Relative rotative efficiency	1.0	–
η_s	Shaft efficiency	0.98	–
ρ_A	Air density	1.225	kg/m ³
ρ_W	Seawater density	1025	kg/m ³

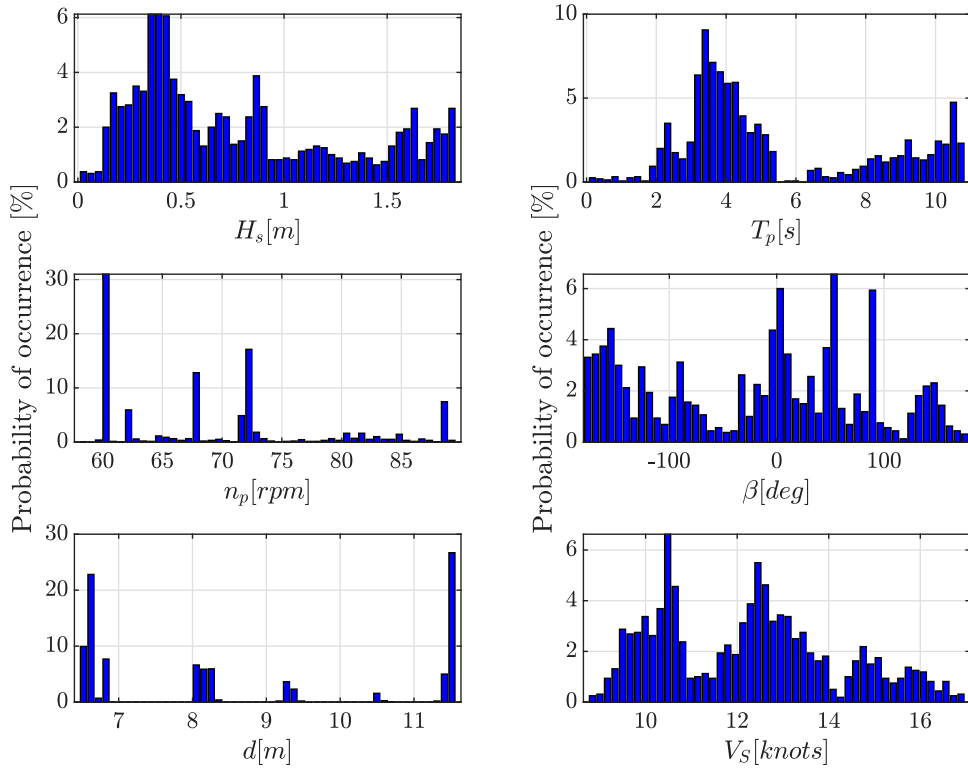


Figure 3. The scatter plots of different input features from the general cargo ship's processed data across M1V1.

integers are given in Table 5, and the bound limits are determined by how many candidate methods are being considered for each component.

It is worth noting that surrogate optimization can be applied to problems with both integer and continuous bounds. Thus, the proposed method can be valuable for problems that require tuning specific parameters as well as for finding optimal methods for the power prediction model. The optimization problem is then defined as follows.

$$\text{Decision variables } X = [i_{R_{Calm}}, i_{R_{Wave}}, i_{R_{Wind}}, i_{\eta}, i_{S_{wet}}, i_{C_M}, i_{C_{WP}}]$$

$$\text{Objective min } NRMSE(X, x_{inp})$$

where the input vector $x_{inp} = [x_{data}, x_{const}]$, where $x_{data} = [V_s, n_{rpm}, d, H_s, T_p, \beta]$ are obtained based on the ship in-service data and weather hindcast data. In addition, x_{const} represents the constant parameter vector as given in Table 6. The optimization algorithm searches for the most suitable integer that corresponds to the optimal method for each component of the power prediction model from a total of $6 \times 3^2 \times 2^4 = 864$ possible power prediction models.

The proposed power prediction method is trained based on 1600 data points for a voyage of the ship within Mission 1 called M1V1 (Mission 1, Voyage 1). Scatter plots of different input features across M1V1 are shown in Figure 3. Figure 4 shows that for most parts of the studied voyage, GPS and log speeds are quite similar. Therefore, the effects of the sea current have been disregarded in the analysis.

Figure 5 illustrates a simple schematic of implementing the proposed power prediction method for the studied general cargo ship. Through this process, Model 1 is obtained. The worst power prediction model, Model 2, is obtained by specifying the optimization objective as the negative value of NRMSE. Here, the percentage of NRMSE, $NRMSE_{pc}$, is defined as $NRMSE_{pc} = NRMSE \times 100$. It is found that the best combination, Model 1, reached the $NRMSE_{pc}$ of 4.72%, while the worst combination of methods, Model 2, reaches the $NRMSE_{pc}$ of 33.73%, indicating an 86% percentage difference between the results achieved through the worst and the best combinations. The results indicate that the error difference between the two models is largely due to the difference in the propulsion system efficiency.

The details of the obtained models by the tuning optimization algorithms are provided in Table 7. Except for S_{wet} , C_M , and C_{WP} , other hydrostatic parameters are calculated numerically through the ship offset table for Model 2. However, for Model 1, they are all calculated numerically through the ship offset table. It is primarily the geometric input parameters and the efficiency of the propulsion system that determine the difference between the worst and best models for this problem. An interesting point about the results is that as a result of the different input parameters and combination effects, Holtrop, CTH, and ISO 15016 are both in the category of the best and the worst models (Model 1 and Model 2) with about an 86% percentage difference in the NRMSE results. These results clearly

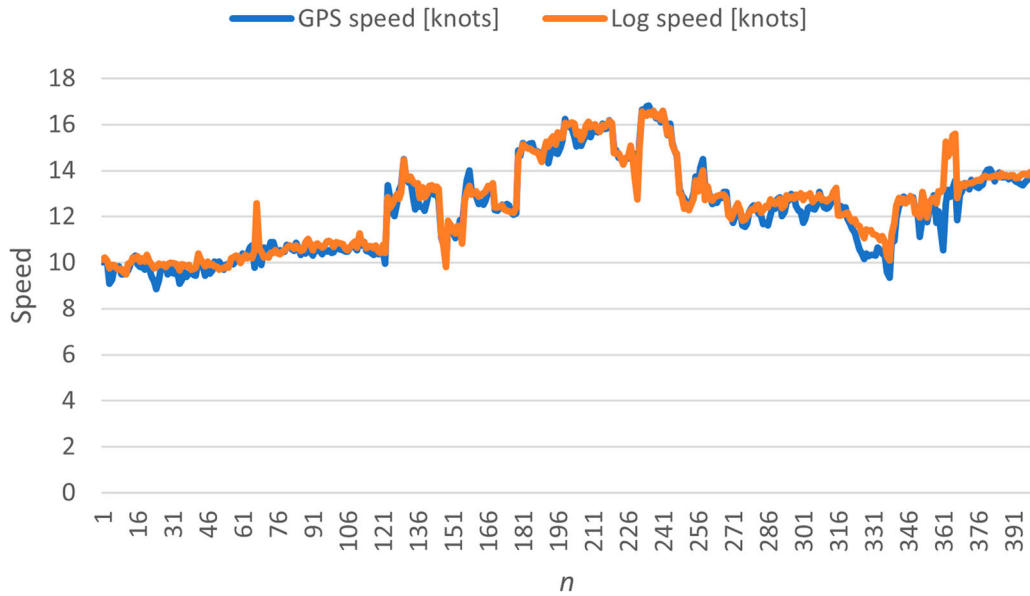


Figure 4. Log speed against GPS speed across M1V1.

demonstrate that the input parameters and the combination effect among various methods and parameters have a significant impact on the accuracy of the power prediction model, and emphasize the value of

the proposed method when it comes to improving the accuracy of a power prediction model. In addition, calculating open-water efficiency through B-series propellers, the most common method compared to other

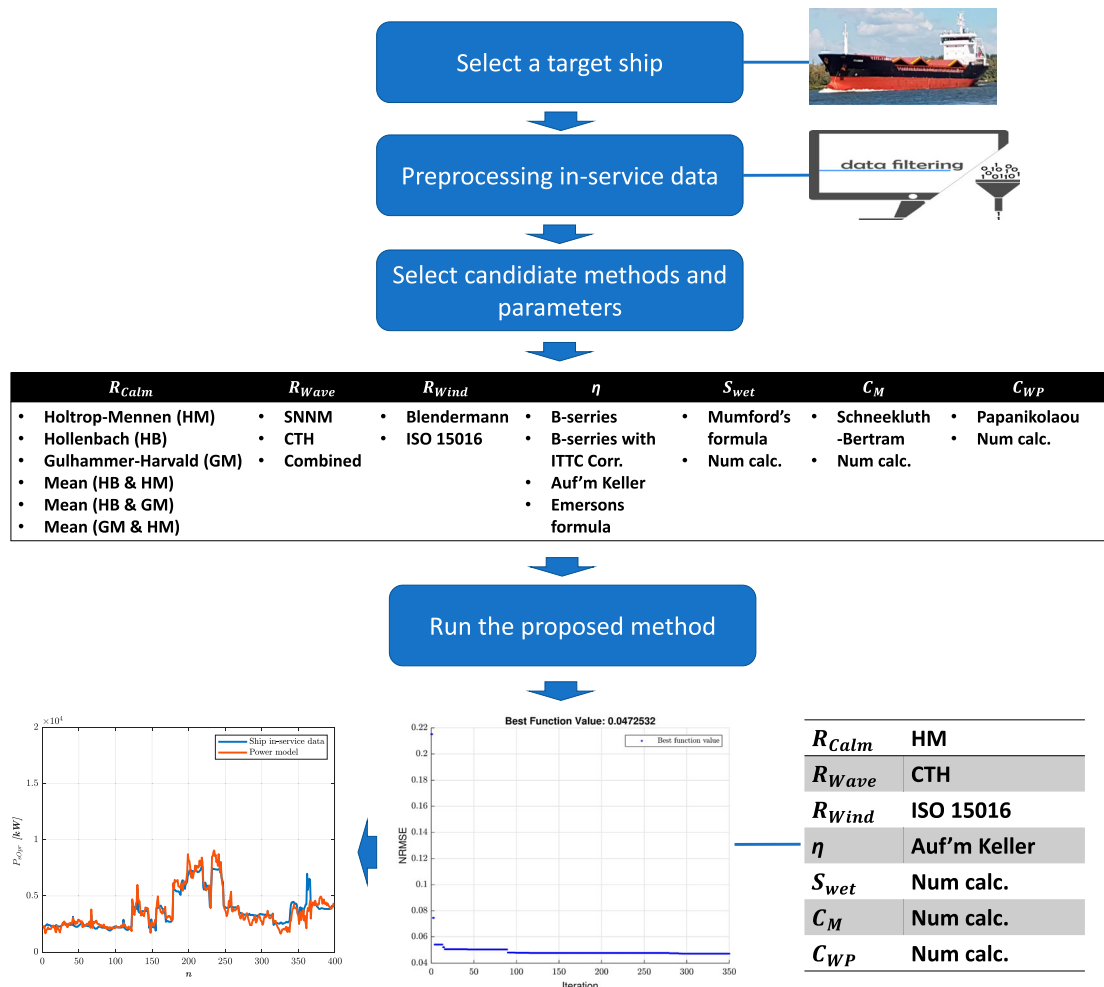


Figure 5. A simple schematic of implementing the proposed method for the studied general cargo ship.

Table 7. The results of the tuning algorithms for different models.

	Model 1 (optimum)	Model 2 (worst combination)
R_{Calm}	Holtrop-Mennen	Holtrop-Mennen
R_{Wave}	CTH	CTH
R_{Wind}	ISO 15016	ISO 15016
η	Auf'm Keller	B-series
S_{wet}	Numerical computation	Mumford's formula
C_M	Numerical computation	Schneekluth and Bertram
C_{WP}	Numerical computation	Papanikolaou

studied methods falls into the worst power prediction category for the studied ship. These results show that assumptions used for developing power prediction methods can have a considerable negative effect on the accuracy of the prediction, and the proposed method can be useful for evaluating those assumptions.

The results of the power prediction models for the different models in the studied operational condition (M1V1) are shown in Figure 6. The results for Model 1 indicate the high performance of the proposed approach in decreasing the inaccuracy of the model in most operating points. The worst model, however, shows a poorer performance in the majority of the conditions.

The tuning data obtained from M1V1 corresponds to a short-term voyage of a ship. However, a ship might experience different weather conditions on different voyages during her mission. Therefore, it is necessary to evaluate the efficiency of power prediction models across different voyages the ship might encounter. Here, a test data set of 800 samples with a time interval of 15 minutes from a different voyage across Mission 1 (referred to as M1V2 (Mission 1, Voyage 2)) is employed for testing the performance of the resulting models. Scatter plots of the different input features across M1V2 are presented in Figure 7. The comparison of Figures 3 and 7 shows that the ship experiences higher significant wave heights and mostly operates in the ballast draft in M1V2, while other input features fall within the range of M1V1 with a different distribution. The results are presented in Figure 8. It can be seen that Model 1 keeps its high performance in M1V2 while Model 2 still shows relatively poor performance. Also, the $NRMSE_{pc}$ of Model 1 and Model 2 are 3.78% and 27.16%, respectively, indicating an 88% percentage difference in the $NRMSE_{pc}$ of the two models.

4. Comparison analyzes

4.1. Comparison with artificial neural network (ANN)

Perhaps the most popular machine learning technique for sophisticated data-driven (black-box) models is artificial neural networks. ANN is composed of three layers, including an input layer, one or more hidden

layers, and an output layer. Each node, or artificial neuron, is connected to others and has a corresponding weight and threshold. If the node output exceeds a predefined threshold value, it is activated and starts transferring data to the next layer. Otherwise, no data is sent to the network's next layer. The procedure used for implementing the ANN used in this study is described below.

- (i) Data preprocessing: Here, we use the same in-service data as we did in the previous section for the proposed method.
- (ii) ANN main parameters: For the purpose of comparing the ANN model with the proposed method, ANN power prediction models are developed in this study. Thus, the same input variables and outputs as the proposed method are also used here. As a result, ship speed over ground (SOG), mean draught, significant wave height, mean wave period, and wave encounter angle are the input variables and shaft power is the output variable. For the training of the ANN model, typical ranges of hyperparameters used in ANN are considered, as shown in Table 8, and the optimal combination of parameters within the range is selected through the grid search (Pedregosa et al. 2011). Here, the n_{rpm} has not been included as an input in the ANN model due to the strong correlation between V_S and n_{rpm} . This decision might be based on the rationale to avoid multicollinearity, which can affect the reliability of the estimates in the model.
- (iii) Model implementation and validation: This step sought to implement the ANN power prediction model using pre-processed data and the ANN main parameters obtained from the previous step. The M1V1 (Mission 1 Voyage 1) is used as the training voyage.

Running ANN yields an $NRMSE_{pc}$ of 5.33% for the training data, which is slightly higher than that of the suggested approach (4.72%). We can see that the models obtained through the ANN and the proposed methods have quite similar prediction performance and perform well for the training data. To further compare the performance of these two methods, it is interesting to see how they perform for different data sets. This is accomplished by evaluating the ANN's and proposed method's sensitivity to different voyages, missions, sampling time intervals, and lengths of time history. The results of the comparison between the predicted propulsion power by the proposed approach (Model 1) and ANN against the measured power for the test voyage (M1V2) are shown in Figure 9. The results of ANN for the test dataset indicate an $NRMSE_{pc}$ value of 4.29%, which is also slightly greater than that of the suggested

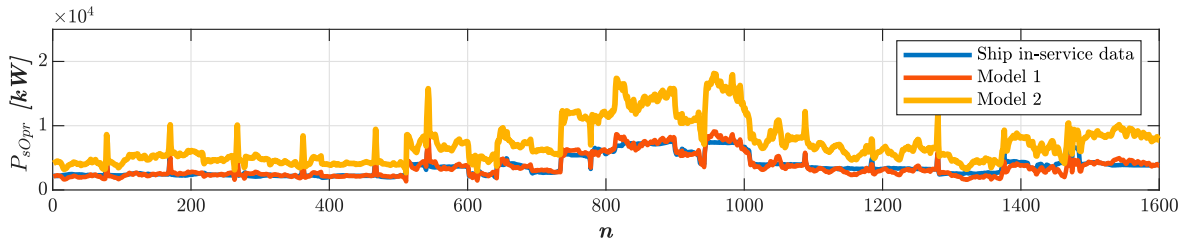


Figure 6. The comparison between the shaft power predicted by Model 1 and Model 2 against the measured power across M1V1.

approach, which is 3.78%. Therefore, both the proposed approach and ANN perform well in predicting ship power, while the suggested approach performs slightly better. As a further comparison between the proposed approach and ANN, the effects of the change in the sampling interval and the ship mission are also provided in the upcoming sections.

4.1.1. Sensitivity of models to different missions

In the context of the market, the ship owner's decision, etc., a ship might change her mission. Here, different power prediction models will be compared for a new mission (Mission 2) presented in Figure 10. 3000 samples from Mission 2, representing a one-month voyage of the ship, are considered for studying the performance of the power prediction models. This voyage is referred to as M2V1 (Mission 2, Voyage 1). Because

Mission 2 is longer than Mission 1, more samples have been considered for M2V1. The scatter plots of different input features across M2V1 are shown in Figure 11. Comparing Figure 11 with Figures 3 and 7 reveals that the ship is encountering higher significant wave heights and drafts in M2V1 than in M1V1 and M1V2. The results show that the ANN, the proposed method (Model 1), and Model 2 experience $NRMSE_{pc}$ of 9.4%, 5.07%, and 46.82%, respectively. Figure 12 compares the shaft power predicted by different power prediction models against the measured power across M2V1. In comparison with the previously studied voyage and mission, the results of M2V1 indicate a considerably higher increase in the $NRMSE_{pc}$ for the ANN and Model 2 compared to the proposed approach, implying that the proposed approach has shown more performance robustness

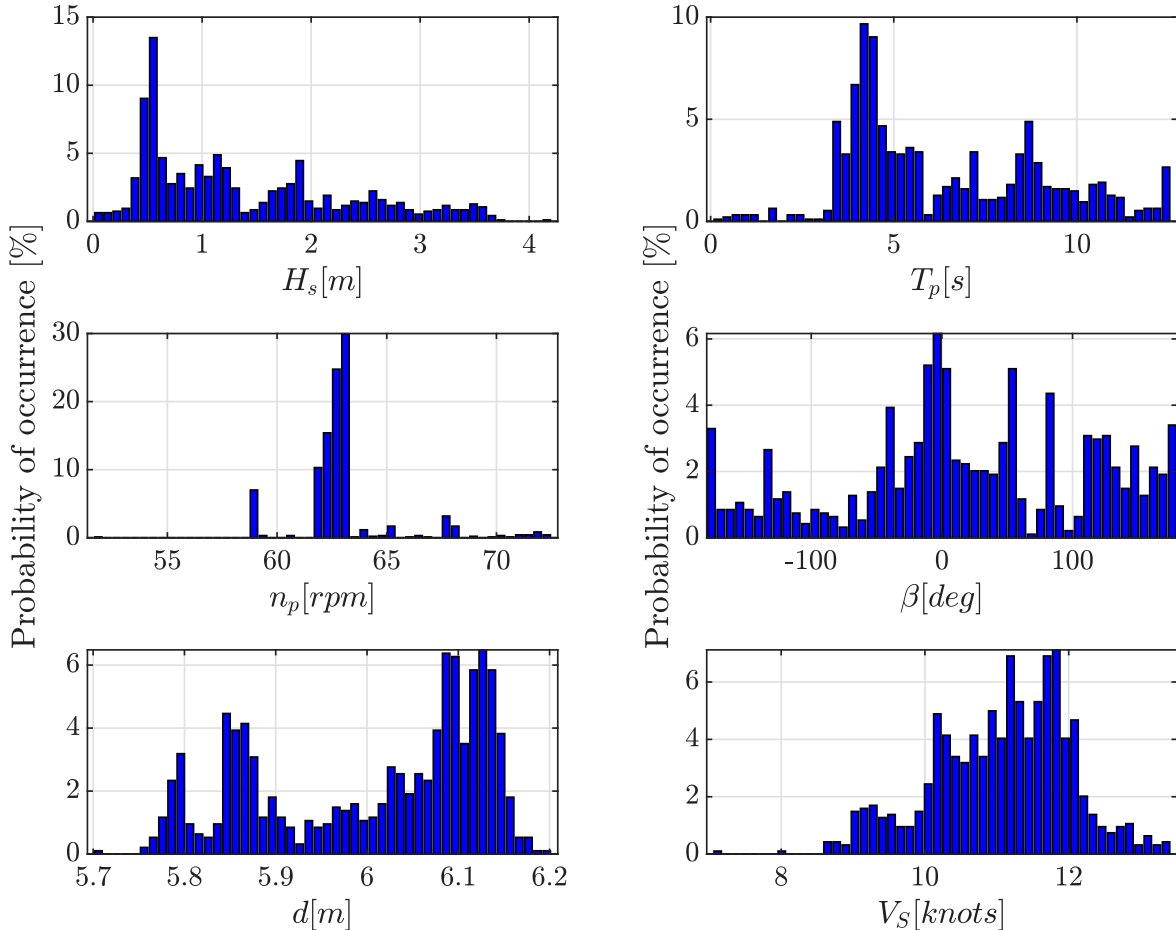


Figure 7. The scatter plots of different input features from the general cargo ship's processed data across M1V2.

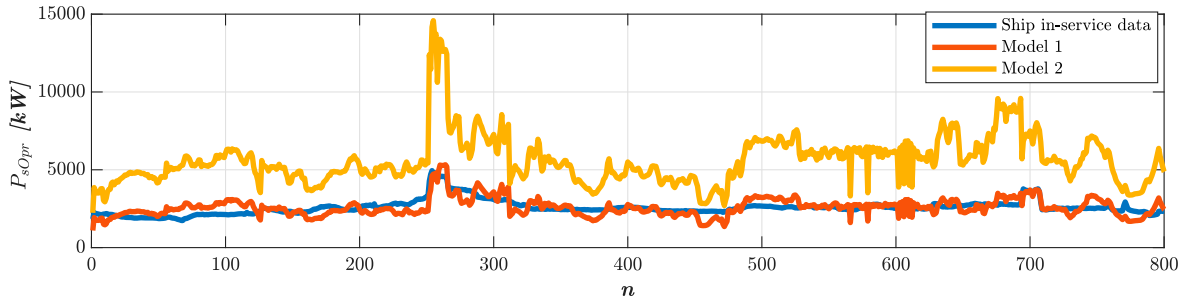


Figure 8. The comparison between the shaft power predicted by Model 1 and Model 2 against in-service measured power across the test voyage (M1V2).

under the changes in the mission and voyage. These results also emphasize the advantage of a physics-based approach (Model 1) over a machine-learning approach in which its performance can be negatively affected by data outside of the trained set. However, it might not always be the case. If the physics-based model is not carefully developed, it might lead to even worse results, as Model 2 did. But this issue can be addressed using the proposed approach.

4.1.2. Sensitivity of models to the sampling time interval

Data for the studied ship is available with a sampling time interval of 15 minutes. Power prediction methods, particularly machine learning methods whose results are directly dependent on data, might perform differently depending on the sampling interval. Thus, it is of interest to evaluate the robustness of power prediction models at different sampling intervals. This is accomplished by running the proposed approach and ANN on training data with sampling intervals of 15 minutes, 30 minutes, 1 hour, 2 hours, and 4 hours. The results for the sampling time interval of 15 minutes have already been obtained. The performance of the resultant models is then assessed for the test voyages (M1V2 and M2V1).

Table 9 presents the NRMSEs of different models obtained by the ANN and the proposed methods at different sampling time intervals. According to these results, both ANN and proposed methods present quite similar prediction accuracy and perform well at each sampling time interval. To assess the

prediction performance of these models across different test voyages, Figure 13 is provided. Comparing the results of the ANN for the training data and the test voyage of M1V2 in Table 9 and Figure 13 reveals a relative increase in the NRMSE in the test voyage with sampling time intervals, indicating the negative effects of increasing the sampling time interval on the performance of the ANN. While for the test voyage of M2V1, the effects of the mission change are more significant than the sampling time interval. Therefore, the sampling interval and mission change can significantly affect ANN performance, while the proposed method shows more robustness, indicating another advantage of the suggested strategy over a machine learning approach.

It should be noted that a larger sampling interval means fewer samples and thus less computational time and cost. As a result, the presented approach should be useful for analyzing the performance of fleets with more ships involved. In the optimization process, this might also facilitate the use of methods that require more computational time or examine more parameters than those used in this study.

4.1.3. Sensitivity of models to the length of time history

In practice, if a ship has an automatic data collection system, it is not customary to have lower data rates than 15 minutes. If it does not have an automatic system, the sampling frequency is usually daily when using the default data rate of 15 minutes. Thus, it is interesting to know how quickly the ANN method will achieve acceptable accuracy. That can be tested by systematically varying the length of time in the training data set. This is done by running the proposed approach and ANN on the training data with the lengths of the time history of $l = 100, 200, 400, 800,$ and 1600 samples collected from the beginning of M1V1. The results for the entire voyage ($l = 1600$) have already been obtained. The resultant models are then evaluated on the test voyages (M1V2 and M2V1). Table 10 shows the models obtained using the proposed approach over different lengths of time history. According to this table, the more data is

Table 8. The main parameters of the ANN model.

Option	Value
Input	5 params (V_s [knots], d [m], H_s [m], T_p [s], β [deg])
Output	1 param (P_s [kW])
Optimizer	Adam
Activation function	ReLU
Loss function	neg mean squared error
Dropout rate	0.1–0.5
Epochs	300–1000
Learning rate	0.001–0.1
Cross validation	5-fold cross validation
No. of hidden layers	1–2
No. of hidden nodes	3–7

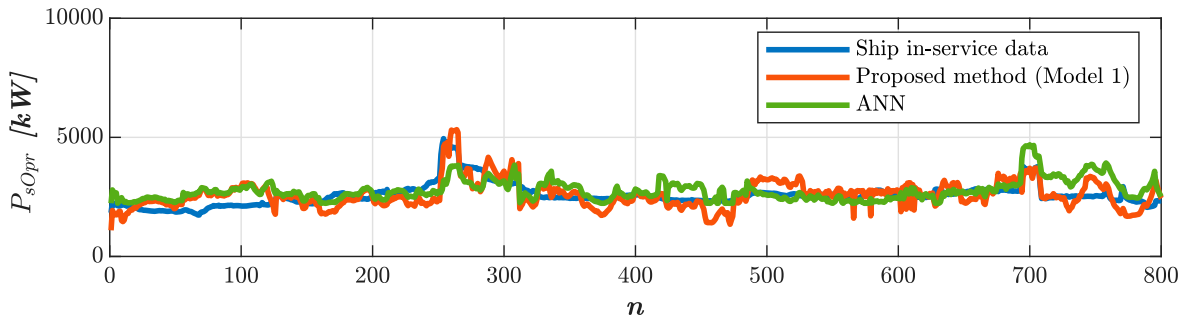


Figure 9. The comparison between the shaft power predicted by the proposed approach (Model 1) and ANN and the measured power across the test voyage (M1V2).

available for the proposed approach, the more similar components of the resultant model are to the best model ($l = 1600$).

Table 11 presents the NRMSEs of different models obtained by the ANN and the proposed methods at different lengths of time history. Based on these results, the models obtained through the ANN and the proposed methods show quite similar prediction accuracy and work well at each length of time history. To evaluate the prediction performance of these models across different test voyages, Figure 14 is provided. The results of test voyages in Figure 14 show that different models developed based on the suggested approach still perform well in predicting ship power across different lengths of time history. The results of the ANN test voyages, however, show poor performance until the length of the time history of 800. These results indicate the robustness of the proposed approach

compared to ANN in the presence of the change in the length of time history.

In some applications, the number of tuning samples in the proposed approach needs to be reduced due to computation time and cost constraints. Comparing the results in this section with those in Section 4.1.2 suggests that the proposed approach might yield better models if the number of samples is reduced by increasing sampling time intervals rather than reducing the length of time history; this is because the data tend to cover a wider range of ship operation profiles and weather conditions.

4.2. Comparison with traditional power prediction models

Toward energy-efficient shipping, an accurate prediction of the ship performance at sea is crucial.

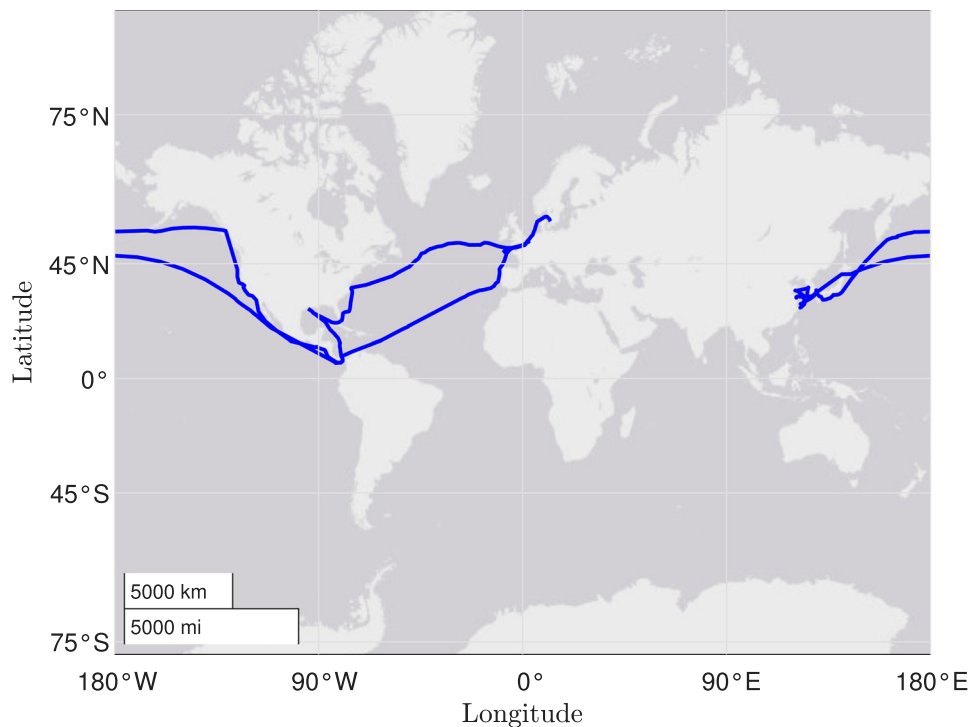


Figure 10. The ship operational route for Mission 2.

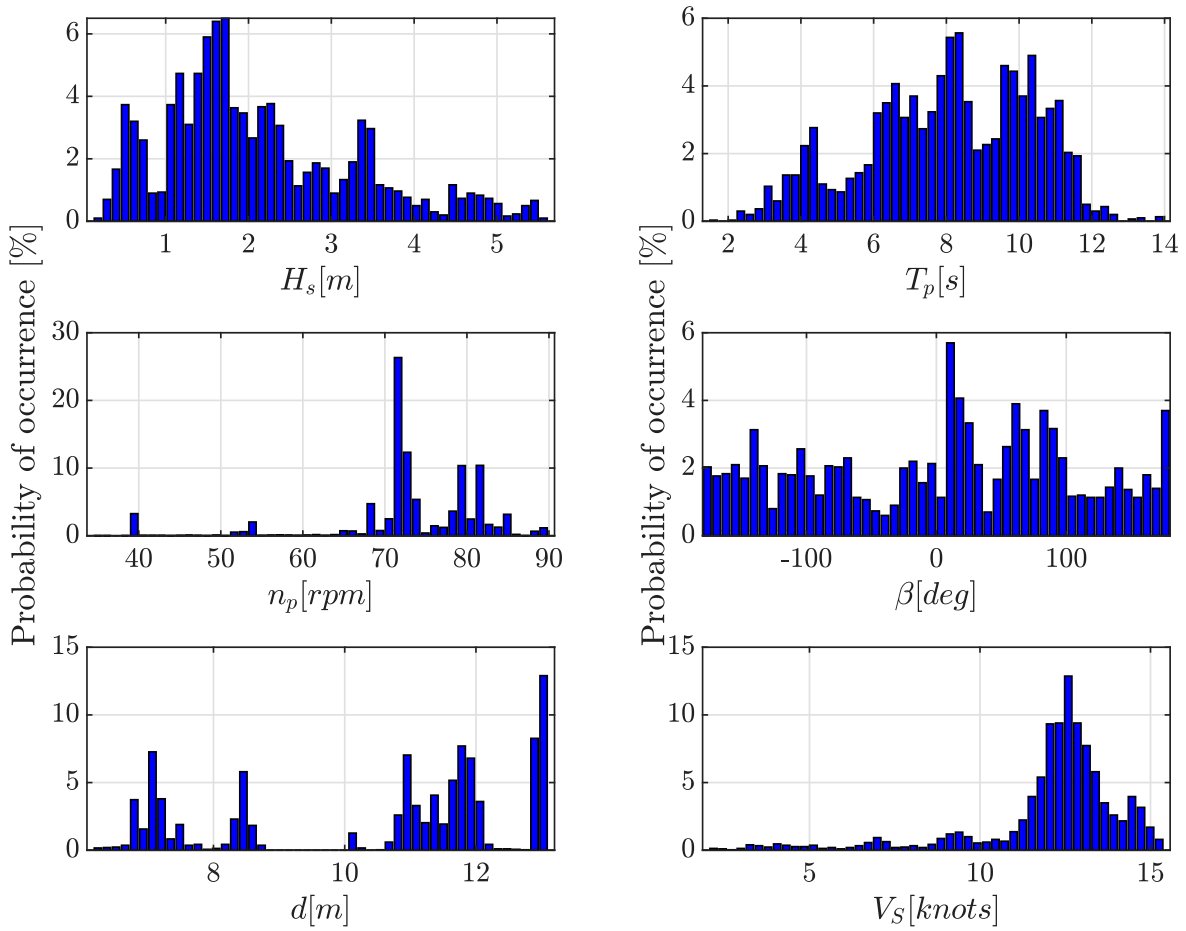


Figure 11. The scatter plots of different input features from the general cargo ship's processed data across M2V1.

Previous power prediction models are built on pre-determined and presumable techniques. The power prediction model's performance, however, may vary significantly depending on the ship type and the operational scenarios. Here, the aim is to compare the results of three traditional methods, i.e., Lindstad et al. (2013), Kristensen et al. (2017), and Johansson et al. (2017), with the suggested methodology. In the following sections, a brief

explanation of those approaches is given, followed by a comparison with the recommended strategy and the ship in-service data.

4.2.1. Kristensen et al. (2017)

The power prediction approach proposed by Kristensen et al. (2017) uses regression estimations for the input parameters using already-established empirical formulae. In the original ITTC 1957

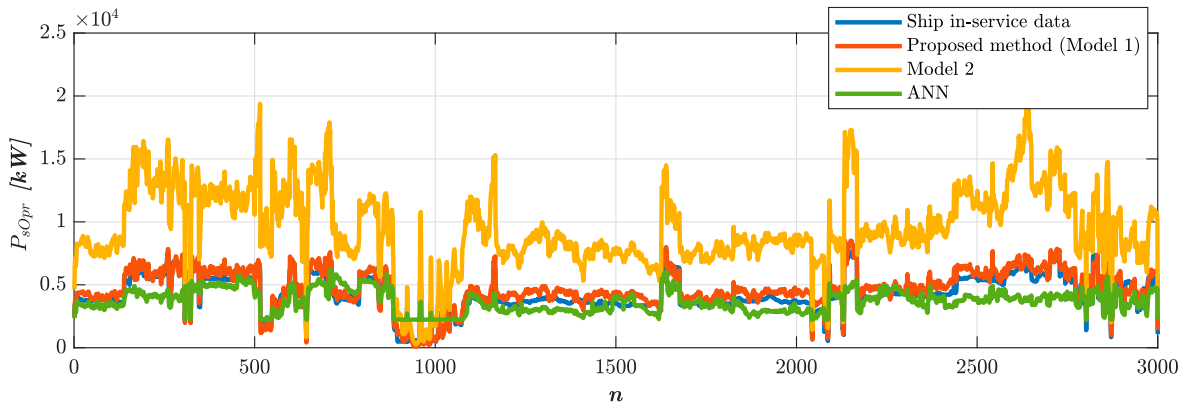


Figure 12. The comparison between the shaft power predicted by different power prediction models against the measured power across M2V1.

Table 9. A comparison of the NRMSEs of the ANN and proposed models developed based on the training data with different sampling time intervals.

	Sampling time interval (Δt)				
	15 min	30 min	1 hr	2 hr	4 hr
ANN	0.0533	0.0415	0.042	0.0344	0.0368
Proposed method	0.0472	0.0474	0.0473	0.0460	0.0473

approach, the total resistance coefficient is expressed as

$$C_T = C_F + C_A + C_{AA} + C_R$$

where C_F , C_A , and C_R are the frictional resistance coefficient, correlation allowance, and residual resistance coefficient, respectively. The ITTC 57 friction line (ITTC 2014) is used to estimate frictional resistance, and the Harvald's approach (1983) is employed to calculate wave-making resistance. Also, the total power is defined as follows.

$$P_{tot} = \frac{R_T \cdot V_S}{\eta_P} \cdot \left(1 + \frac{\text{service allowance in \%}}{100} \right)$$

The service allowance includes wind and wave effects, which are suggested to be in the range of 20–35% depending on the operational region. The study offers new estimates for the thrust deduction fraction and wake factor in addition to a novel technique for doing bulbous bow corrections. Mumford's formula is used to calculate the wetted surface area. Also, a regression analysis on Mumford's formula for 129 modern ships was conducted

to obtain more accurate formulae for the wetted surface depending on the ship type and size. The open water efficiency is calculated using an approximated version of the Wageningen B-series.

4.2.2. Johansson et al. (2017)

Johansson et al. (2017) suggested a power prediction model known as STEAM3. The ITTC friction line and Hollenbach's method are used to calculate the calm-water resistance components (R_F and R_R). The Kwon approach (Kwon 2008) is applied to estimate the added weather resistance. Moreover, Emerson's formula (Campana et al. 2009) is used to calculate the quasi-propulsive efficiency.

4.2.3. Lindstad et al. (2013)

In Lindstad et al. (2013), the following formula is suggested to calculate the ship total power.

$$P_{tot} = K(P_{Calm} + P_{AW} + P_{Wind}) + P_{aux}$$

where P_{Calm} , P_{AW} , P_{Wind} , and P_{aux} are the calm water power, added power in waves, added power due to wind, and auxiliary power, respectively. Also, the

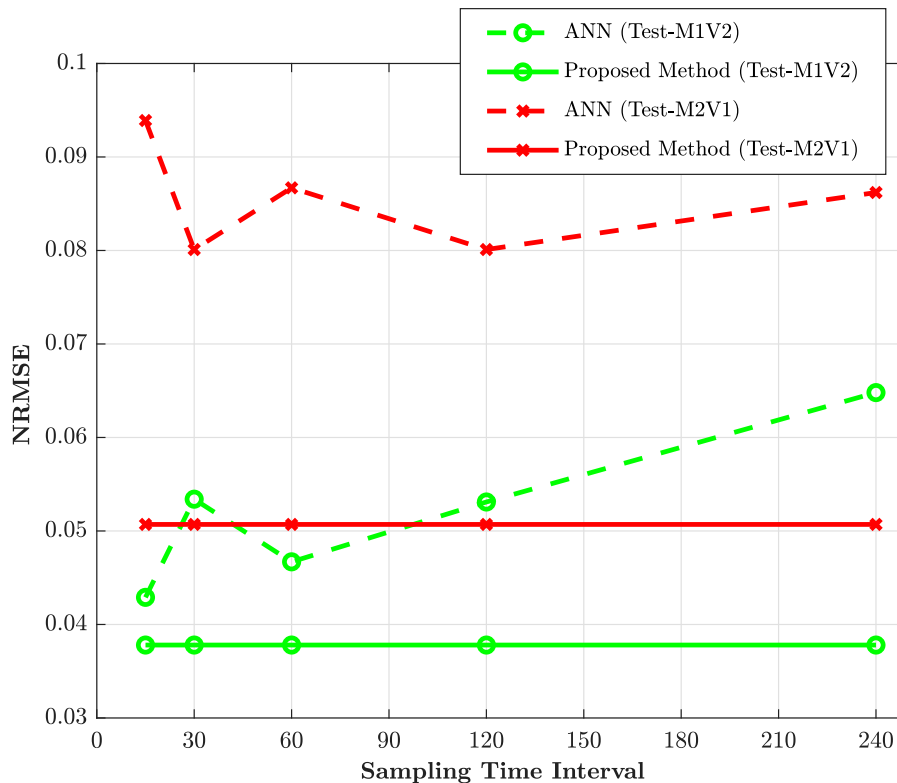
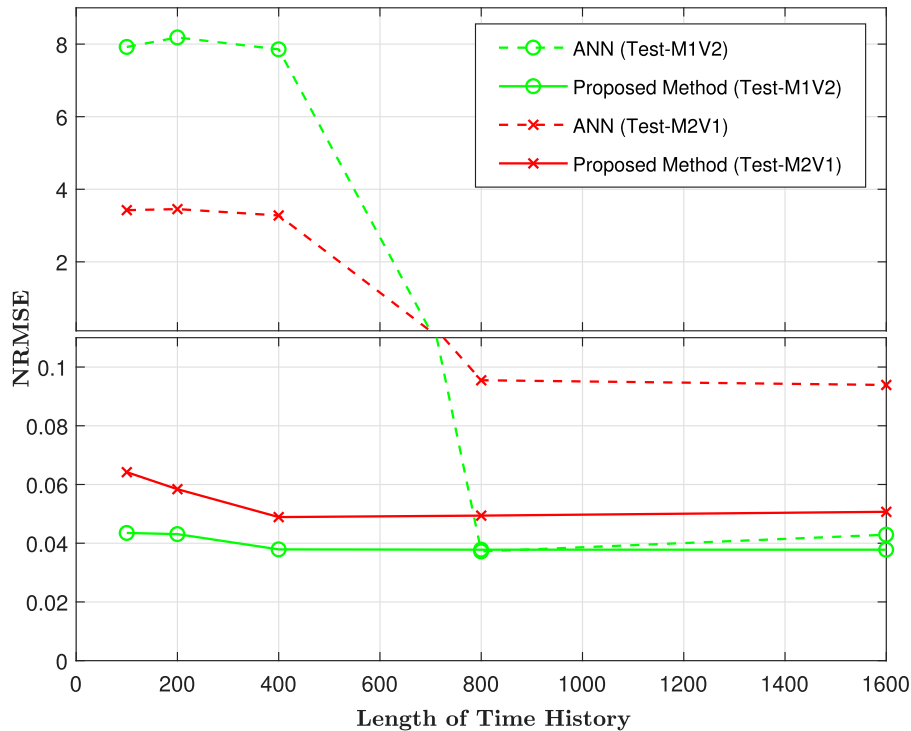
**Figure 13.** A comparison of the NRMSEs of the ANN and the proposed models developed at different sampling time intervals across various test voyages.

Table 10. The models obtained for different lengths of time history through the proposed method.

	Length of time history (<i>l</i>)				
	100	200	400	800	1600
Calm water resistance	HM & GH	HM & GH	HM	HM	HM
Added resistance in wave	CTH	SNNM	Combined	Combined	CTH
Added resistance in wind	ISO 15016	ISO 15016	ISO 15016	ISO 15016	ISO 15016
Propulsion system efficiency	Auf'm Keller	Auf'm Keller	Auf'm Keller	Auf'm Keller	Auf'm Keller
Wetted surface area	Numerical computation	Numerical computation	Numerical computation	Numerical computation	Numerical computation
Midship section coefficient	Schneekluth and Bertram	Schneekluth and Bertram	Numerical computation	Numerical computation	Numerical computation
Waterplane area coefficient	Numerical computation	Numerical computation	Papanikolaou	Numerical computation	Numerical computation

Table 11. A comparison of the NRMSEs of the ANN and proposed models developed based on the training data with different lengths of time history.

	Length of time history (<i>l</i>)				
	100	200	400	800	1600
ANN	0.0145	0.0129	0.016	0.0301	0.0533
Proposed method	0.0293	0.0258	0.0268	0.0311	0.0472

**Figure 14.** A comparison of the NRMSEs of the ANN and the proposed models developed at various lengths of time history across different test voyages. To better present the comparison, the y-axis has broken between 0.11 and 1.

coefficient of K is adjusted to account for the impacts of waves on the sea state and corrected for voluntary speed losses as follows.

$$K = \eta(V_s, H_s) = \max\left(\frac{1}{\eta_D(j + k \cdot \sqrt{\frac{V_s}{V_d}})}, \frac{1}{\eta_D(1 - r \cdot H_s)}\right)$$

Holtrop-Mennen (HM), STAWAVE-1, and ITTC methods are used to compute P_{Calm} , P_{AW} , and P_{Wind} ,

respectively. The following constants are applied: $\eta_D = 0.7$, $j = 0.7$, $k = 0.3$, and $r = 0.05$. Lindstad's model has been used in several studies to assess the performance of new technologies in reducing ship GHG emissions (Lindstad et al. 2017; Lindstad and Bø 2018; Lindstad et al. 2022a, 2022b).

4.2.4. Results of comparisons

Here, the input parameters that are used in the proposed method are also employed in the conventional power prediction models, with the power being the

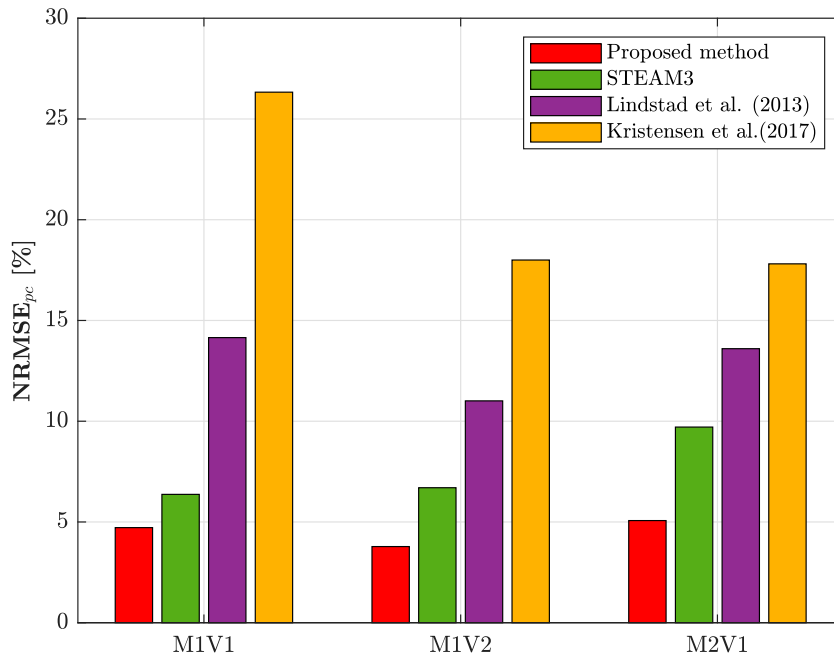


Figure 15. A comparison of NRMSE_{pc} between the proposed method and conventional power prediction models in different operational scenarios.

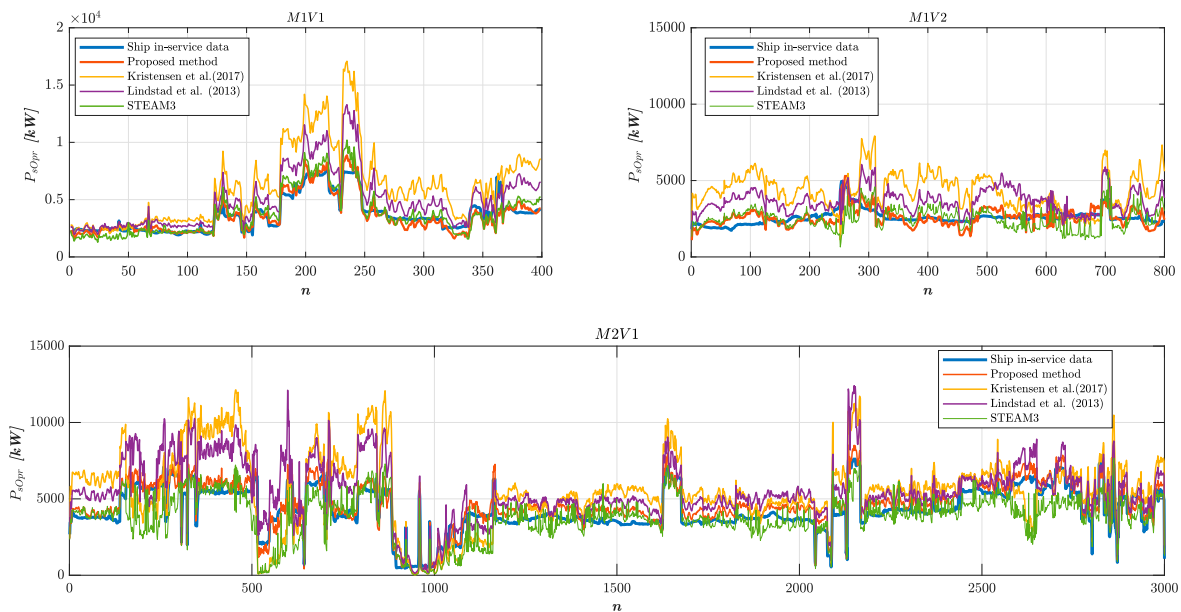


Figure 16. A comparison of the shaft power obtained by the proposed approach with conventional power prediction models across different operational scenarios.

output. Figure 15 compares the NRMSE_{pc} of the suggested approach to that of traditional power prediction models in various operating conditions. Also, a comparison of the shaft power obtained by the proposed approach with conventional power prediction models across different operational scenarios is shown in Figure 16. These results indicate that the performance of the traditional power prediction methods might vary significantly depending on the ship's operational condition, while the proposed method has maintained its performance with higher accuracy. In light of the crucial importance of improving ship

performance prediction at sea, these results emphasize the importance of using the proposed approach rather than the previously suggested power prediction models that are based on predetermined and presumable formulas.

5. Conclusion

This study suggests a tuning method based on a comparison of ship in-service data for a reference vessel and the result of the power prediction model. To do so, by comparing the results from the power

prediction model with the ship in-service data of a reference vessel, the normalized root mean square error (NRMSE) is computed. Then, a tuning surrogate-based optimization problem is developed to minimize the NRMSE and find the optimal combination of methods and input parameters applied to compute different components of the ship power. We used a general cargo ship operating between Italy and Norway as a test case. The results show that the accuracy of the power prediction model is improved by roughly 86% when comparing the worst and best combinations of approaches. Moreover, Holtrop-Mennen, CTH, and ISO 15016 fall within the categories of both the poorest and best power prediction models, indicating a significant effect of the input parameters and method selection. The test results also confirm the efficiency of the suggested methodology.

The performance of the suggested approach was also assessed throughout different ship voyages, missions, sampling time intervals, and lengths of time history. The recommended approach's robustness in the presence of changing sample intervals and missions was shown compared to the artificial neural network (ANN). The longer the sampling interval, the fewer samples and the lower the computational cost and time. Thus, the presented approach should be useful for analyzing the fleet performance with more ships involved or with only small amounts of in-service available. Additionally, it might facilitate the use of more computationally intensive methods or the analysis of more parameters in the optimization process. Moreover, it was demonstrated that the recommended approach is robust to changing the length of time history when compared to ANN. As the length of time history was reduced, the ANN performed poorly, whereas the proposed approach performed with approximately the same accuracy.

The effectiveness of the proposed method was further demonstrated by comparison with the well-known traditional power prediction methods developed by Kristensen et al., STEAM3 (Johanson et al.), and Lindstad et al. In all operational scenarios tested, the suggested approach showed better performance and accuracy.

In light of the growing number of studies that employ ship in-service data for verification and prediction purposes, we recommend implementing the suggested tuning strategy in order to reach a more accurate power prediction model and quantify the expected prediction accuracy. It would be interesting to assess the effectiveness of the suggested methodology in various ship types and scenario applications in further research. Also, as long as the performance data is accurate and covers a large enough range of

variation in the involved parameters, the technique might be applied to other types of performance data than in-service data.

Furthermore, it is interesting to include machine learning techniques in the tuning approach in future studies. Based on the user's decision, the proposed approach can be expanded to incorporate more parameters and methods than those used in this study to provide even better results. Also, the user might need to change candidate methods, parameters, and even assumptions used in this study to achieve the expected accuracy. It is also interesting to include the parameters of the empirical methods in the proposed tuning method to develop better semi-empirical methods for a given case.

If the in-service data for a similar ship is available, the proposed approach might be used in the early design phase of a new ship. However, the sensitivity of the accuracy of the proposed approach to changes in the ship design has not been investigated yet, but is of interest as a topic for further work.

The ship behavior at sea might change over the long term due to factors such as fouling, wear and tear of the propulsion system, etc. Additionally, this might influence the accuracy of the resultant power prediction model on a long-term basis. In this case, classifying the data over different time periods and implementing the proposed approach for each classification might improve the accuracy of the power prediction model over the long term.

Disclosure statement

No potential conflict of interest was reported by the author(s).

CRedit authorship contribution statement

Ehsan Esmailian: Conceptualization, Methodology, Investigation, Software, Writing – Original Draft. **Young-Rong Kim:** Software, Investigation, Review & Editing. **Sverre Steen:** Methodology, Writing – Review & Editing, Supervision. **Kourosh Koushan:** Review & Editing, Supervision.

Funding

The research was conducted at SFI Smart Maritime (WP2), funded by the Research Council of Norway (Grant number 237917), under the Center for Research-based Innovation (SFI) scheme. Also, the authors appreciate Dr. Prateek Gupta for sharing the in-service data used in this study.

ORCID

Ehsan Esmailian  <http://orcid.org/0000-0002-5482-2216>

References

- Besikçi EB, Arslan O, Turan O, Ölçer AI. 2016. An artificial neural network based decision support system for energy efficient ship operations. *Comput Oper Res.* 66:393–401. doi: [10.1016/j.cor.2015.04.004](https://doi.org/10.1016/j.cor.2015.04.004)
- Blendermann W. 1995. Estimation of wind loads on ships in wind with a strong gradient, OMAE. Copenhagen. *ASME.* p. 271–277
- Brown IN, Aldridge MF. 2019. Power models and average ship parameter effects on marine emissions inventories. *J Air Waste Manage Assoc.* 69:752–763. doi: [10.1080/10962247.2019.1580229](https://doi.org/10.1080/10962247.2019.1580229)
- Campana EF, Peri D, Tahara Y, Kandasamy M, Stern F. 2009. Numerical optimization methods for ship hydrodynamic design. *Transactions-The Society of Naval Architects and Marine Engineers.* 117:30.
- Chassignet EP, Hurlburt HE, Smedstad OM, Halliwell GR, Hogan PJ, Wallcraft AJ, Baraille R, Bleck R. 2007. The hycm (hybrid coordinate ocean model) data assimilative system. *J Mar Syst.* 65:60–83. doi: [10.1016/j.jmarsys.2005.09.016](https://doi.org/10.1016/j.jmarsys.2005.09.016)
- CMEMS. 2018. Monitoring global and center forecasting. Glorys12v1-global ocean physical reanalysis product, eu copernicus marine service information [data set]. <https://resources.marine.copernicus.eu>.
- ECMWF. 2017. Copernicus climate change service (c35). Era5: Fifth generation of ecmwf atmospheric reanalyses of the global climate. Copernicus climate change service climate data store (cds). [accessed 2021 May 8]. <https://cds.climate.copernicus.eu/>.
- Esmailian E, Ghassemi H, Zakerdoost H. 2017. Systematic probabilistic design methodology for simultaneously optimizing the ship hull-propeller system. *Int J Naval Architecture Ocean Eng.* 9:246–255. doi: [10.1016/j.ijnaoe.2016.06.007](https://doi.org/10.1016/j.ijnaoe.2016.06.007)
- Esmailian E, Gholami H, Røstvik HN, Menhaj MB. 2019. A novel method for optimal performance of ships by simultaneous optimisation of hull-propulsion-bipv systems. *Energy Conversion Manage.* 197:111879. doi: [10.1016/j.enconman.2019.111879](https://doi.org/10.1016/j.enconman.2019.111879)
- Faltinsen OM. 1980. Prediction of resistance and propulsion of a ship in a seaway. *Proceedings of the 13th Symposium on Naval Hydrodynamics, Tokyo, Japan.* The Shipbuilding Research Association of Japan.
- Grin R. 2015. On the prediction of wave-added resistance with empirical methods. *J Ship Production Design.* 31:181–191. doi: [10.5957/jspd.2015.31.3.181](https://doi.org/10.5957/jspd.2015.31.3.181)
- Guldhammer H, Harvald SA. 1974. Ship resistance-effect of form and principal dimensions.(revised). Danish Technical Press, Danmark, Danmarks Tekniske Højskole, kademisk Forlag, St. kannikestrade 8, DK 1169 Copenhagen.
- Gupta P, Rasheed A, Steen S. 2022. Ship performance monitoring using machine-learning. *Ocean Eng.* 254:111094. doi: [10.1016/j.oceaneng.2022.111094](https://doi.org/10.1016/j.oceaneng.2022.111094)
- Gupta P, Taskar B, Steen S, Rasheed A. 2021. Statistical modeling of ship's hydrodynamic performance indicator. *Appl Ocean Res.* 111:102623. doi: [10.1016/j.apor.2021.102623](https://doi.org/10.1016/j.apor.2021.102623)
- Harvald SA. 1983. Resistance and propulsion of ships. New York, NY: Wiley.
- Hollenbach KU. 1998. Estimating resistance and propulsion for single-screw and twin-screw ships-ship technology research 45 (1998). *Schiffstechnik.* 45:72.
- Holtrop J. 1984. A statistical re-analysis of resistance and propulsion data. *Int Shipbuilding Progress.* 31:272–276.
- ISO. 2015. ISO 15016:2015-ships and marine technology – guidelines for the assessment of speed and power performance by analysis of speed trial data. Geneva: ISO.
- ITTC. 2014. 1978 ITRC performance prediction method. Recommended Procedures and Guidelines.
- Johansson L, Jalkanen JP, Kukkonen J. 2017. Global assessment of shipping emissions in 2015 on a high spatial and temporal resolution. *Atmos Environ.* 167:403–415. doi: [10.1016/j.atmosenv.2017.08.042](https://doi.org/10.1016/j.atmosenv.2017.08.042)
- Kim B, Kim TW. 2017. Weather routing for offshore transportation using genetic algorithm. *Appl Ocean Res.* 63:262–275. doi: [10.1016/j.apor.2017.01.015](https://doi.org/10.1016/j.apor.2017.01.015)
- Kim YR, Esmailian E, Steen S. 2022. A meta-model for added resistance in waves. *Ocean Eng.* 266:112749. doi: [10.1016/j.oceaneng.2022.112749](https://doi.org/10.1016/j.oceaneng.2022.112749)
- Kim YR, Jung M, Park JB. 2021. Development of a fuel consumption prediction model based on machine learning using ship in-service data. *J Marine Sci Eng.* 9:137. doi: [10.3390/jmse9020137](https://doi.org/10.3390/jmse9020137)
- Kim YR, Steen S, Kramel D, Muri H, Strømman AH. 2023. Modelling of ship resistance and power consumption for the global fleet: the mariteam model. *Ocean Eng.* 281:114758. doi: [10.1016/j.oceaneng.2023.114758](https://doi.org/10.1016/j.oceaneng.2023.114758)
- Kitamura F, Ueno M, Fujiwara T, Sogihara N. 2017. Estimation of above water structural parameters and wind loads on ships. *Ships Offshore Struct.* 12:1100–1108. doi: [10.1080/17445302.2017.1316556](https://doi.org/10.1080/17445302.2017.1316556)
- Koboević Ž., Bebić D, Kurtela Ž.. 2019. New approach to monitoring hull condition of ships as objective for selecting optimal docking period. *Ships Offshore Struct.* 14:95–103. doi: [10.1080/17445302.2018.1481631](https://doi.org/10.1080/17445302.2018.1481631)
- Kristensen HO, Lützen M. 2012. Prediction of resistance and propulsion power of ships. *Clean Shipping Currents.* 1:1–52.
- Kristensen HO, Lützen M, Bingham HB. 2017. Prediction of resistance and propulsion power of ships (Work Package 2, Report no. 4). Technical Report. Technical University of Denmark.
- Kwon Y. 2008. Speed loss due to added resistance in wind and waves. *Nav Archit.* 3:14–16.
- Lang X, Mao W. 2021. A practical speed loss prediction model at arbitrary wave heading for ship voyage optimization. *J Marine Sci Appl.* 20:410–425. doi: [10.1007/s11804-021-00224-z](https://doi.org/10.1007/s11804-021-00224-z)
- Lee JB, Roh MI, Kim KS. 2021. Prediction of ship power based on variation in deep feed-forward neural network. *Int J Naval Archit Ocean Eng.* 13:641–649. doi: [10.1016/j.ijnaoe.2021.08.001](https://doi.org/10.1016/j.ijnaoe.2021.08.001)
- Lindstad E, Bø TI. 2018. Potential power setups, fuels and hull designs capable of satisfying future eedi requirements. *Transp Res Part D: Transport Environment.* 63:276–290. doi: [10.1016/j.trd.2018.06.001](https://doi.org/10.1016/j.trd.2018.06.001)
- Lindstad E, Dražen P, Rialland A, Sandaas I, Stokke T. 2022a. Reaching imo 2050 ghg targets exclusively through energy efficiency measures. *SNAME Maritime Convention.* OnePetro.
- Lindstad E, Polić D, Rialland A, Sandaas I, Stokke T. 2022b. Decarbonizing bulk shipping combining ship design and alternative power. *Ocean Eng.* 266:112798. doi: [10.1016/j.oceaneng.2022.112798](https://doi.org/10.1016/j.oceaneng.2022.112798)
- Lindstad H, Asbjørnslett BE, Jullumstrø E. 2013. Assessment of profit, cost and emissions by varying speed as a function of sea conditions and freight market. *Transp Res Part D: Transport Environment.* 19:5–12. doi: [10.1016/j.trd.2012.11.001](https://doi.org/10.1016/j.trd.2012.11.001)

- Lindstad HE, Eskeland GS, Riialand A. 2017. Batteries in offshore support vessels—pollution, climate impact and economics. *Transp Res Part D: Transport Environment*. 50:409–417. doi: [10.1016/j.trd.2016.11.023](https://doi.org/10.1016/j.trd.2016.11.023)
- Liu S, Papanikolaou A. 2020. Regression analysis of experimental data for added resistance in waves of arbitrary heading and development of a semi-empirical formula. *Ocean Eng*. 206:107357. doi: [10.1016/j.oceaneng.2020.107357](https://doi.org/10.1016/j.oceaneng.2020.107357)
- MathWorks. 2022. Surrogate optimization for global minimization of time-consuming objective functions. [accessed: 2022 May 4]. <https://es.mathworks.com/help/gads/surrogateopt.html>.
- Moreira L, Vettor R, Guedes Soares C. 2021. Neural network approach for predicting ship speed and fuel consumption. *J Marine Sci Eng*. 9:119. doi: [10.3390/jmse9020119](https://doi.org/10.3390/jmse9020119)
- Oosterveld MWC, van Oossanen P. 1975. Further computer-analyzed data of the wageningen b-screw series. *Int Shipbuilding Progress*. 22:251–262. doi: [10.3233/ISP-1975-2225102](https://doi.org/10.3233/ISP-1975-2225102)
- Papanikolaou A. 2014. *Ship design: methodologies of preliminary design*. Dordrecht: Springer.
- Parkes A, Sobey A, Hudson D. 2018. Physics-based shaft power prediction for large merchant ships using neural networks. *Ocean Eng*. 166:92–104. doi: [10.1016/j.oceaneng.2018.07.060](https://doi.org/10.1016/j.oceaneng.2018.07.060)
- Pedregosa F, Varoquaux G, Gramfort A, Michel V, Thirion B, Grisel O, Blondel M, Prettenhofer P, Weiss R, Dubourg V, et al. 2011. Scikit-learn: machine learning in python. *J Mach Learning Res*. 12:2825–2830.
- Perez T. 2006. *Ship motion control: course keeping and roll stabilisation using rudder and fins*. London: Springer Science & Business Media.
- Petersen JP, Winther O, Jacobsen DJ. 2012. A machine-learning approach to predict main energy consumption under realistic operational conditions. *Ship Technol Res*. 59:64–72. doi: [10.1179/str.2012.59.1.007](https://doi.org/10.1179/str.2012.59.1.007)
- Planakis N, Papalambrou G, Kyrtatos N. 2022. Ship energy management system development and experimental evaluation utilizing marine loading cycles based on machine learning techniques. *Appl Energy*. 307:118085. doi: [10.1016/j.apenergy.2021.118085](https://doi.org/10.1016/j.apenergy.2021.118085)
- Saettone S, Tavakoli S, Taskar B, Jensen MV, Pedersen E, Schramm J, Steen S, Andersen P. 2020. The importance of the engine-propeller model accuracy on the performance prediction of a marine propulsion system in the presence of waves. *Appl Ocean Res*. 103:102320. doi: [10.1016/j.apor.2020.102320](https://doi.org/10.1016/j.apor.2020.102320)
- Schneekluth H, Bertram V. 1998. *Ship design for efficiency and economy* (Vol. 218). Oxford: Butterworth-Heinemann.
- Shao W, Zhou P, Thong SK. 2012. Development of a novel forward dynamic programming method for weather routing. *J Marine Sci Technol*. 17:239–251. doi: [10.1007/s00773-011-0152-z](https://doi.org/10.1007/s00773-011-0152-z)
- Shin D. 2021. The effects of explainability and causability on perception, trust, and acceptance: implications for explainable ai. *Int J Hum Comput Stud*. 146:102551. doi: [10.1016/j.ijhcs.2020.102551](https://doi.org/10.1016/j.ijhcs.2020.102551)
- Smith TW, Jalkanen J, Anderson B, Corbett J, Faber J, Hanayama S, O'keeffe E, Parker S, Johansson L, Aldous L, et al. 2015. *Third imo greenhouse gas study 2014*.
- Stewart RH. 2008. *Introduction to physical oceanography*. Texas: Texas A & M University.
- Sun X, Yan X, Wu B, Song X. 2013. Analysis of the operational energy efficiency for inland river ships. *Transp Res Part D: Transport Environment*. 22:34–39. doi: [10.1016/j.trd.2013.03.002](https://doi.org/10.1016/j.trd.2013.03.002)
- Tadros M, Vettor R, Ventura M, Guedes Soares C. 2021. Coupled engine-propeller selection procedure to minimize fuel consumption at a specified speed. *J Marine Sci Eng*. 9:59. doi: [10.3390/jmse9010059](https://doi.org/10.3390/jmse9010059)
- Tillig F, Ringsberg JW, Mao W, Ramne B. 2018. Analysis of uncertainties in the prediction of ships' fuel consumption—from early design to operation conditions. *Ships Offshore Struct*. 13:13–24. doi: [10.1080/17445302.2018.1425519](https://doi.org/10.1080/17445302.2018.1425519)
- Tillig F, Ringsberg JW, Psaraftis HN, Zis T. 2020. Reduced environmental impact of marine transport through speed reduction and wind assisted propulsion. *Transp Res Part D: Transport Environment*. 83:102380. doi: [10.1016/j.trd.2020.102380](https://doi.org/10.1016/j.trd.2020.102380)
- Vernengo G, Gaggero T, Rizzuto E. 2016. Simulation based design of a fleet of ships under power and capacity variations. *Appl Ocean Res*. 61:1–15. doi: [10.1016/j.apor.2016.09.003](https://doi.org/10.1016/j.apor.2016.09.003)
- Wang J, Rakha HA. 2017. Fuel consumption model for heavy duty diesel trucks: model development and testing. *Transp Res Part D: Transport Environment*. 55:127–141. doi: [10.1016/j.trd.2017.06.011](https://doi.org/10.1016/j.trd.2017.06.011)
- Watson DG. 1998. *Practical ship design* (Vol. 1). Oxford: Elsevier.
- Zhang C, Zhang D, Zhang M, Mao W. 2019. Data-driven ship energy efficiency analysis and optimization model for route planning in ice-covered arctic waters. *Ocean Eng*. 186:106071. doi: [10.1016/j.oceaneng.2019.05.053](https://doi.org/10.1016/j.oceaneng.2019.05.053)